An Accurate 3D Localization Technique using a Single Camera and Ultrasound

Masanori Sugimoto Noriyoshi Kanie Shigeki Nakamura
Interaction Technology Laboratory, Dept. of EEIS
University of Tokyo
Tokyo, Japan
{sugi, kanie, shigeki}@itl.t.u-tokyo.ac.jp

Hiromichi Hashizume
Information Systems Architecture Science Research Division
National Institute of Informatics
Tokyo, Japan
has@nii.ac.jp

***Abstract*—We propose a novel technique for 3D localization that integrates a single camera and ultrasound. We use the Extended Phase Accordance Method and the ultrasound to measure accurately the distance to a moving target and we use the camera to identify the target's 2D position on the image plane. A prototype system consists of a transmitter unit mounting one ultrasound transmitter and three infrared LEDs around it, and a receiver unit with one inexpensive camera and one ultrasound receiver. We implemented these units in a lightweight and compact way (receiver unit size: 55 mm × 44 mm), to make the system robust against the no-line-of-sight problems that frequently occur in trilateration or multicamera-based systems. Experimental results show that the RMSEs of the proposed system are 1.20 mm and 1.66 mm for static and mobile (velocity: 1.0 m/s) targets, respectively. These indicate that the performance of the system is comparable with that of high-end systems.**

Keywords: 3D localization technique; integration of ultrasound measurement and camera; accurate ultrasound distance measurement; compact system

I. Introduction

Our group earlier developed and evaluated an ultrasound ranging technique called the Phase Accordance Method (PAM) [1]. PAM is a time-of-flight (TOF) ranging technique and uses two sinusoidal waves with different frequencies. A time reference point called the epoch when the phase difference of the waves becomes zero is set at the transmitter and the epoch is detected at the receiver. In our performance evaluation experiments, PAM achieved 0.032 standard deviations (s.d.) in a three-meter ranging measurement. To the best of our knowledge, PAM achieved the world best ranging performance by using a narrowband ultrasound transducer. By using PAM and its extension, a ranging technique called the Extended Phase Accordance Method (EPAM) [2], our group has implemented a robot tracking system [3], gesture recognition system [4], motion-capture system [5] and other applications.

A 3D positioning system using ultrasound ranging measurements is based on trilateration, which is the positioning principle used by global positioning systems (GPSs). The accuracy of a trilateration-based positioning system depends on (1) ranging accuracy and (2) beacon/sensor geometry (e.g., the relative positions of the satellites in a GPS). As shown in Figure 1, if the sensors are spatially spread, a value related to the geometric dilution of precision (GDOP) is small (good GDOP) and accurate positioning results can be expected [6]. In contrast, when the sensors are densely located, the GDOP value is large (poor GDOP) and the positioning accuracy deteriorates. However, sparsely located sensors have several disadvantages: for instance, the system size becomes large, its deployment becomes difficult, and its portability becomes poor.

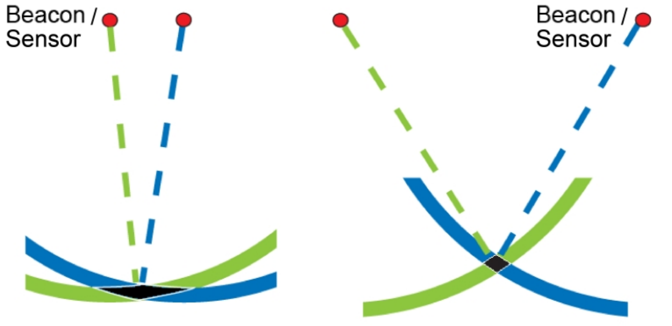

Figure 1: Beacon/sensor geometry. The arrangement in the left figure shows poor GDOP (short baseline between sensors), which causes poorer positioning accuracy, and that in the right figure shows better GDOP (long baseline), which achieves better positioning accuracy.

The 3D positioning system developed by our group [3]–[5] was implemented in a compact way by making the baselines between sensors short. We confirmed that it retained a sufficiently accurate level of positioning. However, through evaluations of these systems, the following problems were identified.

- Phase characteristics of ultrasound transducers

  An ultrasound transducer has its own directivity. Therefore, its phase characteristic depends on the incident and output angles of the ultrasound signals. As PAM detects the epoch by obtaining the phase difference between two sinusoidal waves, the phase characteristics of ultrasound transducers affect their positioning accuracy.

978-1-4673-1954-6/12/$31.00 ©2012 IEEE

- A limitation of 3D positioning accuracy because of poor GDOP

  When the GDOP is poor, small range errors are amplified to large 3D positioning errors [7]. Although the error in the ranging direction is small, that on a plane orthogonal to the ranging direction becomes large, as shown in Figure 1.

In this paper, we use the following two methods to overcome the problems described above and propose an accurate and compact 3D tracking system.

- Compensation for the phase characteristics of the ultrasound transducers
- Integration of camera and ultrasound ranging measurements

To allow the compensation, the phase characteristics of an ultrasound transducer are measured by changing the incident angles of ultrasound signals. Then, a phase characteristic compensation plane is generated using a spline function. To confirm the effects of the compensation quickly, we conduct it only for ultrasonic receivers and not for the transmitters in this study. A camera located close to the ultrasound receiver on a receiver unit captures the position of the transmitter (target) on its image plane. The incident angles of signals from the transmitter are then obtained and the phase compensation of the receiver for ranging is performed.

Experimental results show that root-mean-square errors (RMSEs) of the proposed system are 1.20 mm and 1.66 mm for static and mobile (velocity: 1.0 m/s) targets, respectively. These indicate that the performance of the system is comparable with that of high-end systems.

This paper is organized as follows: In Section II, related work is introduced. Section III describes the details of the proposed system. Experimental results are presented in Section IV. Based on these results, we discuss the merits, limitations and issues that are investigated in Section V. Section VI gives the conclusion.

II. RELATED WORK

There are many studies related to positioning systems using camera-based and ultrasound approaches. However, as the technical novelty in this study is not in the camera, but rather in the ultrasound measurements and the camera and ultrasound integration, only systems and techniques related to ultrasound ranging and positioning are introduced in this section.

Active Bat [8] is an ultrasonic localization system that uses the time-of-arrival (TOA) method. In this system, an ultrasonic transmitter called the bat was attached to each of the targets and ultrasonic receivers were deployed in the environment. Active Bat achieved a median error of 6 cm. The Cricket location support system [9] addresses the privacy issue of the Active Bat by swapping the roles of the ultrasonic devices. This system was extended to the Cricket Compass [10], which could measure the orientation of the target as well as its position. In the Cricket Compass system, the receiver device used five ultrasonic sensors to determine its orientation. The localization error of the Cricket Compass was at best 5 cm. The Cricket's ability to track moving objects was investigated by Smith et al. [11]. They conducted localization experiments using a model train as a target. The median error of localization was at best 4 cm when the model train was moving at 1.43 m/s.

McCarthy et al. [12] proposed an algorithm to calibrate the beacons of their localization system automatically. With their algorithm, the beacons can be placed at arbitrary positions. The standard deviation of the measured horizontal coordinates was reported to be 1.1 cm. Wenderberg et al. [13] discussed a method for self-localizing multiple passive receiver nodes using the time-difference-of-arrival (TDOA) method. They devised a nonlinear algorithm called the cone alignment algorithm and reported 2.5 cm RMSEs. Minami et al. [14] proposed a novel distributed algorithm to determine the positions of nodes automatically with minimal manual configuration. The system guided a user to conduct manual preconfigurations of only a few reference nodes. It then estimated the positions of all the other nodes by using a recursive positioning algorithm.

Hazas et al. [15] developed a localization system called Dolphin. The Dolphin transmitters modulated ultrasonic signals using Gold codes, which made the system more accurate and scalable. The localization error was reported to be within 2.5 cm. Saad et al. [16] devised a ranging technique using a wideband frequency-hop spread-spectrum signal. For robust and accurate measurements, a two-step TOF detection method using cross-correlations between transmitted and received signals and phase shift calculations was proposed. Using a wideband signal as in these two approaches allows accurate ranging or localization more easily than a narrowband signal. However, these approaches are not applicable to the proposed system using narrowband ultrasound transducers. Huang et al. [17] designed a transmission signal including two sequential pulses having a phase difference of 180° (phase inversion). By analyzing the interference caused by the phase inversion in the output signal of a receiver and finding a zero response in its amplitude, the TOF of the signal was correctly identified.

Misra et al. [18] improved the Cricket system [9] to extend its measurable area. Three ultrasound transducers were placed in a dodecahedron arrangement to make the receiver unit omnidirectional. Obertholzer et al. [19] proposed a system called SpiderBat by arranging four ultrasonic transmitters and four receivers in a circle interchangeably. SpiderBat was reported to be robust against multipath and no-line-of-sight (NLOS) problems.

III. PROPOSED SYSTEM

A. 3D positioning using camera and ultrasound measurements

Figure 2 shows the configuration of the proposed system. An ultrasound receiver and a camera are mounted on the receiver unit of the system. The target to be located is augmented with an ultrasound transmitter and a visual marker; the marker's position is to be recognized by the camera. The target position (x, y, z) can be found by using the following three equations:

$$\frac{x_i}{f} = \frac{x}{z}, \quad \frac{y_i}{f} = \frac{y}{z}, \quad x^2 + (y-l)^2 + z^2 = d^2, \qquad (1)$$

where l is the length of the baseline between the ultrasound receiver and camera, f is the focal length of the camera, (x_i, y_i) is the position of the target on the image plane of the camera, and d is the distance to the target from the ultrasound receiver.

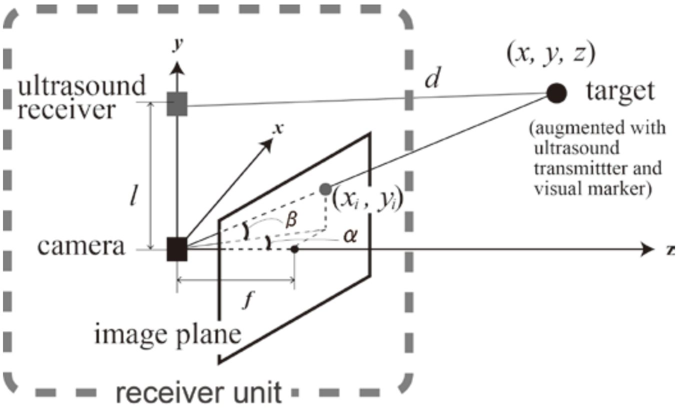

Figure 2: 3D localization using a camera and ultrasound transducers.

B. Extended Phase Accordance Method (EPAM)

As briefly described in Section I, EPAM was extended from PAM to identify the velocity and position of a moving target accurately. The transmitted signal of EPAM has two parts (Figure 3). The first part is a burst signal called a sync pattern for identifying the distance to the target. A sync pattern is a beat signal composed of two ultrasonic sinusoidal waves with different frequencies. The epoch, the unique time point at which the phase difference of the waves becomes zero in the signal, is used as a reference point to determine the signal propagation time between the transmitter and the receiver. Detecting the epoch using EPAM is described below.

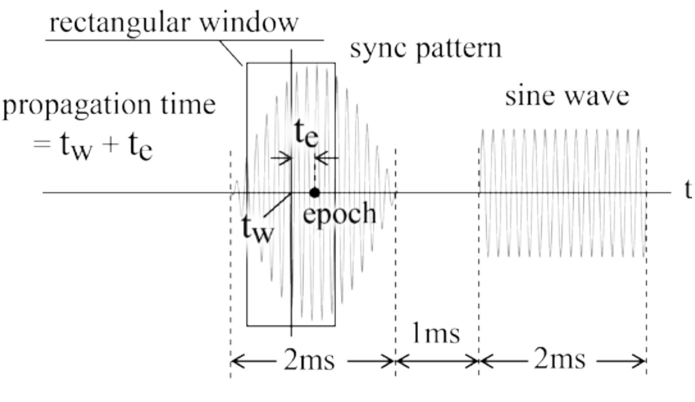

Figure 3: Transmitted signal for the Extended Phase Accordance Method.

Mathematically the sync pattern is expressed as:

$$\begin{aligned} s_d(t) &= a_1 \sin(\omega_1 t + \phi_1) + a_2 \sin(\omega_2 t + \phi_2) \\ &= a_1 \sin(2\pi f_1 t + \phi_1) + a_2 \sin(2\pi f_2 t + \phi_2), \end{aligned} \qquad (2)$$

where a_1 and a_2 are amplitudes, and $\omega_1 = 2\pi f_1$ and $\omega_2 = 2\pi f_2$ are the angular frequencies of the two sinusoidal waves.

The phases ϕ_1 and ϕ_2 are identified using quadrature detection, and are calculated through the inner products of the sync pattern and the complex exponential functions of the corresponding frequencies.

Let us define the inner product of a sync pattern $s(t)$ and $e^{j\Omega t}$ as:

$$\left\langle s(t), e^{j\Omega t} \right\rangle = \frac{1}{T}\int_{-T/2}^{T/2} (t)\, e^{j\Omega t}\, dt = I + jQ\,. \qquad (3)$$

In this equation, time T is an integration interval and frequency Ω is called a reference angular frequency. When the reference angular frequencies are ω_1 and ω_2, we obtain the equations below by inner products as discussed in [1].

$$\begin{aligned} a_1\, e^{j\phi_1} &= 2j\left\langle s(t), e^{j\omega_1 t} \right\rangle \\ a_2\, e^{j\phi_2} &= 2j\left\langle s(t), e^{j\omega_2 t} \right\rangle \end{aligned} \qquad (4)$$

The amplitudes a_1 and a_2 and the phases ϕ_1 and ϕ_2 of the sync pattern are obtained by calculating the real and imaginary parts of the equations. To identify the epoch, the time delay t_e in Figure 3 is calculated by using Equation (5):

$$t_e = \frac{\phi_1 - \phi_2}{\omega_1 - \omega_2}\,. \qquad (5)$$

When the target is static, the distance between the transmitter and the receiver is obtained by multiplying the velocity of sound by the signal propagation time ($t_w + t_e$) in Figure 3. t_w is the midpoint in time of a rectangular window for conducting the quadrature detection represented as Equation (3).

However, when the target is moving, the angular frequencies ω_1 and ω_2 change because of the Doppler effect. The second part of the transmitted signal in Figure 3 is a single sinusoidal wave for identifying the velocity of the target, and thus measuring the Doppler-shifted frequency. It is represented as Equation (6) below:

$$s_v(t) = a_0 \sin(\omega_0 t + \phi_0) = a_0 \sin(2\pi f_0 t + \phi_0) \qquad (6)$$

In EPAM, the shifted frequency is calculated by using the fact that the amplitude a_0 is not affected by the Doppler effect. This means that when two inner products of the Doppler-shifted signal $s_v(t)$ (its angular frequency changes from ω_0 to $\omega_0^{'}$) and $e^{j\Omega t}$, where the reference angular frequencies are ω_1 and ω_2, calculated by using Equations (4), the amplitude a_0 obtained from these inner products must have the same value. This method is faster and more accurate (s.d.: 0.78 mm/s) than conventional methods using the Fourier transform [2].

For the implementation of EPAM, we used an inexpensive narrowband ultrasound transducer with a center frequency of 40 kHz. The sync pattern was generated by two sinusoidal waves with frequencies of 39.75 kHz (= f_1) and 40.25 kHz (= f_2) and lasts 2 ms. The single sinusoidal wave with a frequency of 40.0 kHz (= f_0) follows the sync pattern and lasts 2 ms.

C. Compensation for phase characteristics of ultrasound transducers

Because of the directivity of an ultrasound transducer, its amplitude and phase characteristics depend on the incident and output angles of signals. As EPAM uses the phase information of a sync pattern for ranging, the phase characteristics of ultrasound transducers seriously affect their ranging performance and should be compensated. To clarify the effects of the compensation in this study, we measured the phase characteristics of an ultrasound receiver by changing the incident angles of incoming signals from known positions.

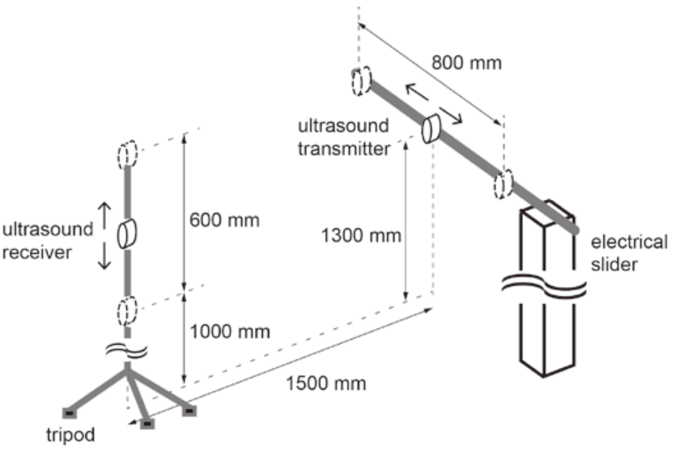

Figure 4: An environment for measuring phase characteristics of an ultrasound receiver.

The measurement environment shown in Figure 4 was configured as follows. The vertical position of the ultrasonic receiver sensor (Nippon Ceramic Co Ltd, RX-16) was changed from 1000 mm to 1600 mm above the floor in 30-mm steps using a tripod. The horizontal position of an ultrasound transmitter (Nippon Ceramic Co Ltd, TX-16) 1300 mm above the floor was changed from –400 mm to 400 mm in 40-mm steps using an electrical slider (Oriental Motor, SPVL8M150UA). The shortest distance between the transmitter and the receiver was 1500 mm. In total, 441 (= 21 × 21) locations of the receiver, covering ±11.3° horizontally and ±8.5° degrees vertically from the transmitter were measured. At each location, 30 measurements were conducted and the average s.d. of phases of all 441 location measurements was 4.32×10^{-3} rad, which corresponds to 0.46 mm. Figure 5 shows a compensated curved surface obtained by using the ranging data at the 441 grid points interpolated using a B-spline function. The figure clearly shows that ranging errors caused by the phase characteristics are small when the incident angle is small. However, the error increases as the angle increases. In addition, the compensation curved surface is not smooth and predictable, but rather is complicated and unpredictable. Thus, we must investigate further how many grid points are required to compensate the phase characteristics to sufficient accuracy.

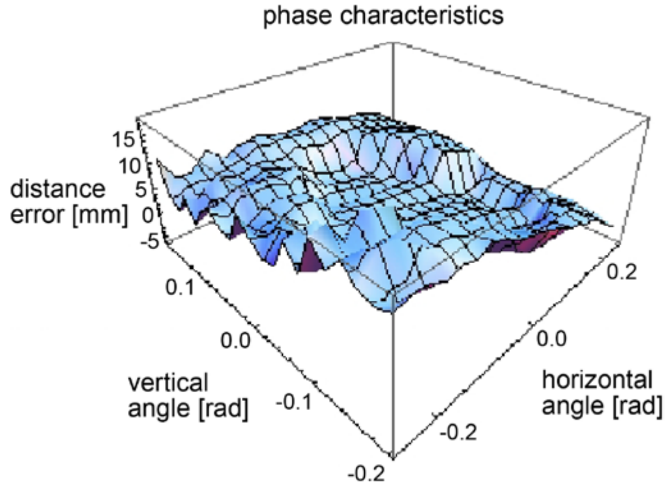

Figure 5: Compensation surface from ultrasound ranging measurements and B-spline interpolation.

From Figure 2, it is clear that α and β are not the correct incident angles to the ultrasound receiver, because the camera and the receiver are separated by the baseline length l. Thus, the compensation for the phase characteristics of the receiver is conducted by finding the correct angles, as follows.

1. Find $\alpha = \tan^{-1}\frac{x}{z}$ and $\beta' = \tan^{-1}\frac{y-l}{\sqrt{x^2+z^2}}$ using Equation (1).
2. Update d by conducting the phase characteristic compensation using α and β'.
3. End if d changes by less than a threshold amount, otherwise return to 1.

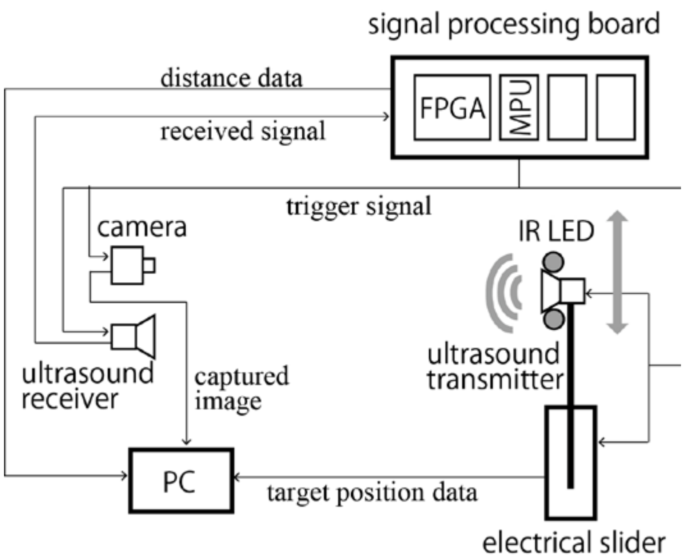

Figure 6: Experimental setup.

IV. EXPERIMENTS

A. *Experimental setup*

To evaluate the performance of the proposed system, the following two experiments were conducted.

- Experiment 1: Static-target localization with and without phase characteristic compensation
- Experiment 2: Moving-target tracking with and without phase characteristic compensation

The purpose of Experiment 1 is to confirm the effects of the compensation by placing a target so that the incident angles to and distances from the receiver are different from those in Section III-*C*. Experiment 2 is designed to evaluate the tracking performance of the proposed system by changing the target velocity.

Figure 6 shows the configuration of the experimental equipment. First, the MPU on the signal processing board sends a trigger signal to the ultrasonic transmitter (target), receiver and the camera (Point Grey, Firefly MV, 1328 × 1048 pixels). At the same time, the transmitter transmits the ultrasound signal and the camera captures an image of the target. The received signal is transferred to the FPGA mounted on the signal processing board for rapid calculation of the ranging measurement results. The transmitter is surrounded by three IR-LEDs as visual markers so that its central point coincides with their geometric center of gravity, as shown in Figure 7. The image obtained by the camera with an IR filter is transferred to the PC and the bright spots of the LEDs are detected at the subpixel level. With the compensated ranging data between the ultrasound receiver and transmitter and the position of the target captured by the camera, the 3D position of the target is identified using Equation (1). The target is mounted on the electrical slider as described in Section III-*C*. The baseline between the camera and ultrasound receiver is set to 27.5 mm (Figure 8). For the calibration of the camera and detection of bright spots, the OpenCV library [20] was used.

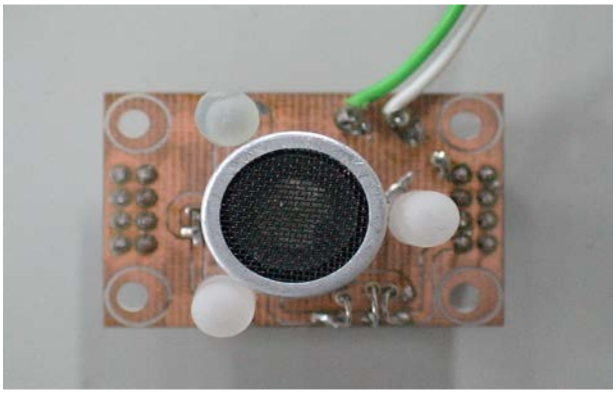

Figure 7: An ultrasound transmitter sensor surrounded by three IR-LEDs as visual markers.

B. *Experiment 1: static-target localization*

The target was placed at eight different positions by controlling the electrical slider on the line orthogonal to the optical axis of the camera. The distance between the target and the receiver was set to 1900 mm. The measurement at each position was conducted 30 times.

Figure 8: A receiver unit including a camera and an ultrasound receiver. Their baseline is 27.5 mm.

Table I shows the experimental results. The results clearly show the advantage of integrating the camera and ultrasound measurements. As discussed in Section I, 3D localization by trilateration with poor GDOP increases positioning errors on a plane (*x*-*y* plane in Figure 2) orthogonal to the ranging direction (*z*-axis in Figure 2). From Table I, it was confirmed that RMSEs, even without compensation, were smaller in the *x*- and *y*-axes than in the *z*-axis because the 2D positioning data obtained by the camera could reduce the ambiguity on that plane. RMSEs with compensation were improved further in all three axes, especially in the *z*-axis, which proved that the phase characteristic compensation worked well to raise the ranging accuracy. The RMSEs of 3D positioning was 1.20 mm, which is close to the performance of recent high-end 3D positioning systems (RMSE: 1 mm or less).

TABLE I. 3D LOCALIZATION OF A STATIC TARGET

	x-axis	*y*-axis	*z*-axis	3D
RMSE without compensation (mm)	1.01	0.31	2.28	2.51
RMSE with compensation (mm)	0.90	0.29	0.74	1.20

C. *Experiment 2: tracking a moving target*

The target mounted on the electrical slider was moved back and forth on the line orthogonal to the optical axis of the camera in the same way as in Experiment 1. The measurement was conducted 179 times with velocity 0.1 m/s and 64 times with velocity 1.0 m/s. Tables II and III show the experimental results.

TABLE II. 3D LOCALIZATION OF A MOVING TARGET (0.1 M/S)

	x-axis	*y*-axis	*z*-axis	3D
RMSE without compensation (mm)	0.92	0.30	2.52	2.70
RMSE with compensation (mm)	0.85	0.28	0.85	1.24

TABLE III. 3D LOCALIZATION OF A MOVING TARGET (1.0 M/S)

	x-axis	*y*-axis	*z*-axis	3D
RMSE without compensation (mm)	0.95	0.32	2.76	2.93
RMSE with compensation (mm)	0.93	0.34	1.34	1.66

The results without compensation confirm that almost the same level of accuracy as that in Experiment 1 was achieved. This indicated that EPAM could accurately identify the distance to the moving target. We also proved that by applying the phase characteristic compensation, the tracking performance was improved. The RMSE of the 3D positioning results at 1.0 m/s was 1.66 mm, which was still comparable with the accuracy of high-end 3D tracking systems.

Figure 9 shows the cumulative distribution functions (CDFs) of the 3D positioning results in Experiments 1 and 2. This figure shows that the phase characteristic compensation worked remarkably well to improve the positioning performance for both static and moving targets. The 90th percentile values with compensations ("w/ comp" in Figure 9) were 2.92 mm, 3.63 mm and 7.23 mm for static, 0.1 m/s velocity and 1.0 m/s velocity targets, respectively, which was improved from 24.3 mm, 26.6 mm, and 23.2 mm ("w/o comp" in Figure 9), respectively.

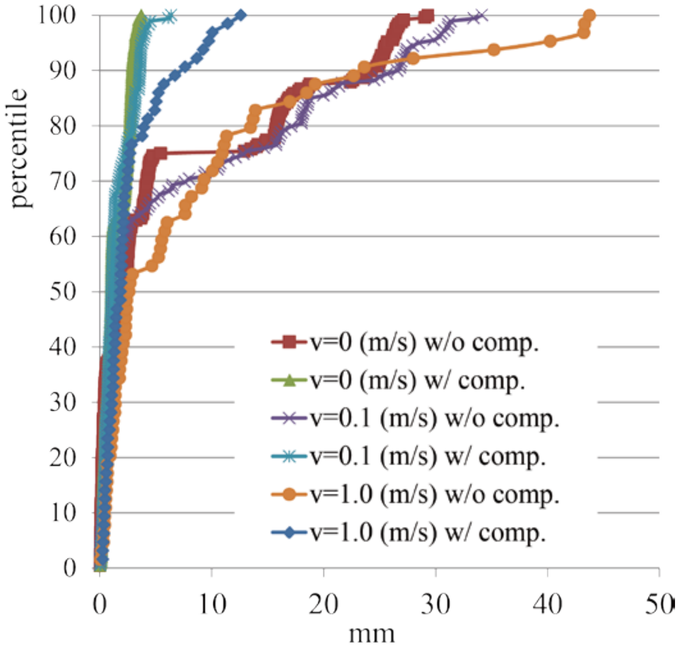

Figure 9: CDFs of the static and tracking experiments.

V. DISCUSSION

A. *Robust and compact 3D tracking system*

Although the proposed system is compact and thus has a poor GDOP, its 3D tracking performance is satisfactory. As discussed in Section I, a 3D positioning system using trilateration with poor GDOP values causes positioning ambiguity on the plane orthogonal to the ranging direction. On the other hand, a 3D positioning system using a stereo camera with poor GDOP increases the level of ambiguity in the ranging direction, as shown in Figure 10. The proposed method combines the merits of ultrasound and camera measurements to improve the accuracy in both the ranging direction and the plane orthogonal to it. Moreover, the improved ranging accuracy of EPAM with the phase characteristic compensation is confirmed to achieve more accurate 3D positioning.

There are advantages related to the compact design of 3D positioning systems with short baselines between sensors. We can reduce the deployment cost because there is no need to install multiple, distributed sensor units in a measurement environment. The portability of the system is also increased. Furthermore, when sensors are spread spatially, the probabilities of 3D positioning failures increase because NLOS to a target from any sensor makes positioning impossible. However, a compact positioning system like the proposed system is more robust to occlusions that cause NLOS than conventional dispersed systems and this can reduce the probabilities of positioning failures.

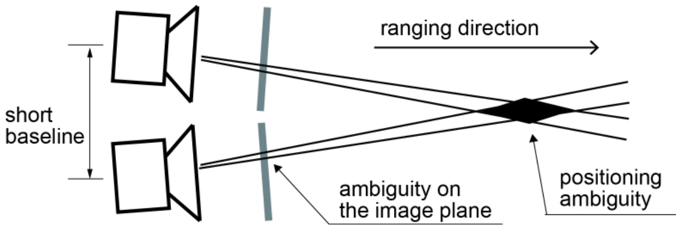

Figure 10: Localization by using a stereo camera. The ambiguity in the ranging direction becomes larger than localization by trilateration (see also Figure 1).

B. *Extension of tracking area*

Because of the attenuation of ultrasound signals propagating in air, measuring the distance to a remote target (e.g., more than 5 m) is often difficult. In addition, the ultrasound transducers used in this paper have relatively strong directivity (FWHM: 55°). Thus, the measurable orientation from the receiver is limited, which is also applicable to a camera. To overcome this problem, using a wide-angle or omnidirectional transducer and camera should be considered.

C. *Transmitter compensation*

In this paper, phase characteristic compensation for an ultrasonic receiver was performed. However, this compensation should be applied not only to the receiver but also to the transmitter. We have already confirmed that compensating radiation patterns of transmitters improves the quality of ultrasound imaging [21]. Thus, we plan to extend our proposed system by including both transmitter and receiver compensation.

D. *Application to motion-capture system*

The experimental results indicate that the proposed system can achieve 3D localization performance comparable with recent expensive motion-capture systems that use multiple high-speed/high-resolution cameras [22] or electromagnetic signals [23]. The current version of our system can track only one target. Therefore, by increasing the number of targets that can be tracked, it may be possible to implement a more flexible motion-capture system integrating ultrasound and camera measurements. The most critical point of this implementation is related to the update rate: how to localize multiple targets rapidly. The dominating factor for the update rate is the ultrasound measurements rather than the camera measurements. EPAM requires 5 ms to transmit one signal, as shown in Figure 3, while a new version of EPAM [24] can reduce the transmission time to 2 ms. Because of the propagation time of sound, about 10 ms is required when the distance between the transmitter and receiver is 3 m. Thus, the theoretical upper limit of the update rate is 100 fps. If a motion-capture system must localize multiple targets, when the number of targets increases, the update rate decreases accordingly with time-division transmission. Thus, to implement a motion-capture or multitarget tracking system, it is better to design it as a passive rather than an active system [11]. By using wideband transmitters, each transmitter can send signals in a different frequency domain so that they do not interfere with each other (frequency-division transmission). As the EPAM was developed originally for a narrowband transducer, it is possible to make the frequency bandwidth for each transmitter narrow, making it easier to increase the number of transmitters simultaneously activated. Embedding different codes into signals from different transmitters to suppress correlations is another option to increase the update rate (code-division transmission).

VI. CONCLUSION

In this paper, we have described a 3D localization technique using a single camera and ultrasound transducers. We use a ranging technique called the Extended Phase Accordance Method to locate stationary or moving targets and compensate for the phase characteristics of ultrasound transducers to make ranging measurements more accurate. Experimental results show that the RMSE of 3D positioning is 1.20 mm for a static target and 1.66 mm for a target moving at 1.0 m/s, which is comparable with recent high-end 3D tracking systems. By combining the merits of ultrasound and camera measurements, the proposed system overcomes problems caused by its compact design (poor GDOP) that affect the positioning performance, and proves that it can conduct accurate target tracking. Future projects are to improve the performance of the proposed system further and to explore the possibilities of applications in industrial fields.

ACKNOWLEDGMENT

This work is supported by Tateishi Science and Technology Foundation and JSPS Grant-in-aid for Scientific Research.

REFERENCES

[1] H. Hashizume, A. Kaneko, Y. Sugano, K. Yatani, and M. Sugimoto: Fast and Accurate Positioning Technique using Ultrasonic PhaseAccordance Method," in *Proceedings of IEEE Region 10 Conference (TENCON2005)*, Melbourne, Australia, pp. 1–6, 2005.

[2] T. Sato, M. Sugimoto, H. Hashizume: An Extension Method of Phase Accordance Method for Accurate Ultrasonic Localization of Moving Node, *IEICE Transactions on Fundamentals of Electronics, Communications and Computer Sciences*, Vol. J92-A, No. 12, pp.953-963, 2009 (in Japanese).

[3] T. Ito, T. Sato, K.Tulathimutte, M. Sugimoto, H. Hashizume: A Scalable Tracking System Using Ultrasonic Communication, *IEICE Transactions on Fundamentals of Electronics, Communications and Computer Sciences*, Vol. E92-A, No.6, pp. 1408-1416, 2009.

[4] S. Nakamura, T. Sato, M. Sugimoto, H. Hashizume: An Accurate Technique for Simultaneous Measurement of 3D Position and Velocity of a Moving Object Using a Single Ultrasonic Receiver Unit, In *Proceedings of IEEE IPIN 2010*, ETH Zurich, Switzerland, pp.1-7, 2010.

[5] T. Sato, S. Nakamura, K. Terabayashi, M. Sugimoto, H. Hashizume.: Design and Implementation of a Robust and Real-time Ultrasonic Motion-capture System, In *Proceedings of IEEE IPIN 2011*, Guimaraes, Portugal, pp.1-6,2011.

(http://ieeexplore.ieee.org/xpl/freeabs_all.jsp?arnumber=6071907)

[6] Y. Lee, Y. Suh, R. Shibasaki.: Ajax GIS Application for GNSS Availability Simulation, *KSCE Journal of Civil Engineering*, Vol. 11, No.6, 303–310, 2007.

[7] P. Misra, B. Burke, M. Prat: GPS performance in Navigation., In *Proceedings of IEEE*, Vol. 87, No. 1, pp. 65–85, 1999.

[8] A. Ward, A. Jones, A. Hopper: A New Location Technique for the Active Office. *IEEE Personal Communications* Vol. 4, No. 5, 42–47, 1997.

[9] N. Priyantha, A. Chakraborty, H. Balakrishnan, H.: The Cricket Location Support System. In *Proceedings of MobiCom2000*, Boston, pp. 32–43, 2000.

[10] N. Priyantha, A. Miu, H. Balakrishnan, S. Teller: The Cricket Compass for Context-aware Mobile Applications. In *Proceedings of MobiCom2001*, Rome, Italy, pp. 1–14, 2001.

[11] A. Smith, H. Balakrishnan, M. Goraczko, M. N. Priyantha: Tracking Moving Devices with the Cricket Location System, In *Proceedings of MobiSys2004*, Boston, MA, pp. 190-202, 2004.

[12] M. McCarthy, P. Duff, H. Muller, C. Randell, C.: Accessible Ultrasonic Positioning. *IEEE Pervasive Computing*, Vol. 5, No. 4, pp. 86–93, 2006.

[13] J. Wendeberg, F. Hoflinger, C. Schindelhauer, L. Reindl: Anchor-free TDOA Self-Localization, In *Proceedings of IEEE IPIN 2011*, Guimaraes, Portugal, pp.1-10, 2011.

[14] M. Minami, Y. Fukuji, K. Hirasawa, K., S. Yokoyama, M. Mizumachi, H. Morikawa, T. Aoyama: DOLPHIN: A Practical Approach for Implementing a Fully Distributed Indoor Ultrasonic Positioning System. In *Proceedings of UbiComp 2004*, Nottingham, UK, pp. 347–365, 2004.

[15] M. Hazas, A. Hopper: Broadband ultrasonic location systems for improved indoor positioning. *IEEE Transactions on Mobile Computing*, Vol. 5, No. 5, 536–547, 2006

[16] M. Saad, C. Bleakley, S. Dobson: Robust High-Accuracy Ultrasonic Range Measurement System, *IEEE Transactions on Instrumentation and Measurement*, Vol. 60, No. 10, pp. 3334-334, 2011.

[17] J. Huang, C. Lee, C. Yeh, W. Wu: High-Precision Ultrasonic Ranging System Platform Based on Peak-Detected Self-Interference Technique, *IEEE Transactions on Instrumentation and Measurement*, Vol. 60, No. 12, pp. 3775-3780, 2011.

[18] P. Misra, S. Jha, D. Ostry: Improving the Coverage Range of Ultrasound-based Localization Systems, In *Proceedings of IEEE WCNC 2011*, Cancun, Mexico, pp. 605-6010, 2011.

[19] G. Oberholzer, P. Sommer, R. Wattenhofer: SpiderBat: Augmenting Wireless Sensor Networks with Distance and Angle Information, In *Proceedings of ACM IPSN 2011*, Chicago, IL, pp. 211-222, 2011.

[20] Open Computer Vision Library Web Site.

http://opencv.willowgarage.com/wiki/.

[21] N. Laokulrat, Y. Maeda, M. Sugimoto, H. Hashizume.: Compensation of a Transmitter's Radiation Pattern for Synthetic Transmit Aperture Acoustic Imaging, In *Proceedings of IEEE IST 2012*, Manchester, UK (2012, to appear).

[22] Vicon: http://www.vicon.com/ (retrieved, July 13th 2012).

[23] Polhermus FASTTRAK:

http://www.polhemus.com/?page=Motion_Fastrak (retrieved, July 13th 2012).

[24] T. Sato, S. Nakamura, M. Sugimoto, H. Hashizume: Extended Phase Accordance Method: A Real-time and Accurate Technique for Estimating Position and Velocity of Moving Objects using Ultrasonic Communication, *Sensors and Transducer Journa*l (special issue, Dec. 2010), Vol.9, pp. 56-70, 2010.